Polymeric Aluminoxanes: A Possible Cocatalytic Support Material for Ziegler–Natta-Type Metallocene Catalysts

CHRISTOPH JANIAK,[1]* BERNHARD RIEGER,[2] RÜDIGER VOELKEL,[3] and HANS-GEORG BRAUN[4]

[1]Institut für Anorganische und Analytische Chemie, Technische Universität Berlin, Straße des 17. Juni 135, D-10623 Berlin, Germany, [2]Institut für Anorganische Chemie, Universität Tübingen, Auf der Morgenstelle 18, D-72076 Tübingen, Germany, [3]Polymer Research Laboratory BASF, Department of Polymer Physics, G201, BASF AG, D-67063 Ludwigshafen, Germany, [4]Polymer Research Laboratory BASF, Department of Polymer Physics, G200, BASF AG, D-67063 Ludwigshafen, Germany.

SYNOPSIS

The reaction of methylaluminoxane (MAO) with 1,6-hexanediol or 1,10-decanediol leads to white powdery materials which were studied by ^{13}C and ^{27}Al MAS NMR, scanning electron microscopy (SEM), and whose surface area and porosity was determined according to the BET method. The hydrolysis of trimethylaluminum with hydrogel was carried out and the product was investigated by SEM. © 1993 John Wiley & Sons, Inc.
Keywords: aluminoxanes • metallocene catalysts, supported

INTRODUCTION

In the 1970s various research groups realized that small amounts of water were capable of raising the activity of the long known Cp_2TiX_2/AlR_2Cl or AlR_3 catalyst system for the polymerization of ethylene.[1,2] Sinn et al.[2] suggested the formation of oligomeric aluminoxanes, e.g., $(MeAlO)_x$.[3] In 1980 Sinn, Kaminsky et al. reported an extremely high activity of the achiral $Cp_2ZrX_2/(MeAlO)_x$ system for the polymerization of ethylene.[4] This together with the pioneering work by Brintzinger et al.[5] on rigid chiral ansa-metallocenes for the production of highly isotactic polypropylene[6] established these metallocene—methylaluminoxane combinations as a new family of catalysts.

While higher-alkyl aluminoxanes are defined compounds, methylaluminoxane (abbreviated MAO) still remains a "black box" despite its uniqueness as a cocatalyst. Few attempts were made to elucidate the MAO structure, e.g., with the help of gel permeation chromatography[7] and NMR.[8] The methylaluminoxane structure can be postulated as being a linear (**1**) or cyclic (**2**) oligomer of MeAlO units:

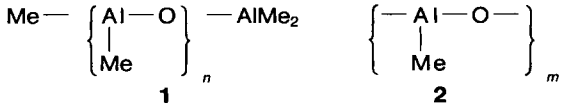

1 **2**

The average molecular weight depends on the preparative conditions. Furthermore, the full cocatalytic functionality of methylaluminoxane is also unknown. A recent IR/NMR study on zirconocene dichloride/MAO systems[9] or an x-ray structure of a neutral dimethylzirconocene/aluminoxane adduct, $\{Cp_2ZrMe(\mu\text{-}OAlMe_2)\}_2$,[10] did not shed much light on this question. The problems in analyzing the methylaluminoxane system arise from the fluctuating, dynamic character of the linear and cyclic oligomers which change their size and structure. Aside from alkylating the metallocene dihalide and being a scavenger for impurities, the cocatalytic function of MAO is probably best described as establishing a stabilizing environment for the metallocene cation or cation–anion pair in the form of a host–guest or "crown-aluminoxane" complex akin to enzymatic catalysis.[11]

There is now widespread academic and industrial interest in these homogeneous metallocene/aluminoxane systems as a potential new generation of

* BASF Postdoctoral Fellow 1990–1991; to whom all correspondence should be addressed.

Journal of Polymer Science: Part A: Polymer Chemistry, Vol. 31, 2959–2968 (1993)
 CCC 0887-624X/93/122959-10

Ziegler–Natta catalysts. As an advantage over the classic heterogeneous Ziegler–Natta catalysts, the metallocene/MAO systems combine high activity with the possibility of tailoring the polymer properties such as molecular weight, molecular weight distribution, comonomer insertion and distribution, as well as tacticity through an *a priori* rational ligand design at the transition metal center.

The sum of these advantages, however, especially the high activity is only obtained, when carrying out the polymerization in homogeneous phase, i.e., in solution—with toluene being the most common solvent. Such a solution polymerization has some inherent drawbacks, though. Besides the usage of large amounts of solvent, there is little control over the morphology of the polymer formed. In a homogeneous system below the polymer melting point, the polymer is obtained as a very fine powder suspended in the polymerization solvent. This not only results in a very high viscosity of the polymerization mixture, but in general, polymers with a particle size of less than about 100 μm create problems upon separation from the reaction medium, upon further handling and storage.[12]

To gain control over the polymer morphology, adsorption of the metallocene/MAO system on a support surface would be the route to follow, in line with the work on the classic heterogeneous Ziegler–Natta catalysts. The polymer particle mimics the initial shape of the catalyst particle, but on a larger scale.[13,14] In addition, the necessary adaption of a new catalyst system to existing plant technologies such as gas phase and slurry phase processes requires heterogenation of the "homogeneous" metallocene/MAO combination.[15] Quite often amorphous silica (silica gel) is employed as a support material for Ziegler–Natta catalysts. The silica is fragmented by the polyolefin as the polymer fills the silica pores during the polymer particle growth and the fragments act as a template for polymer growth.[14] Consequently, silica leads to a good particle size and distribution for a gas phase or slurry process. We recently discussed the support of a zirconocene dichloride/MAO catalyst on silica.[16] A drastic drop in productivity remains the major obstacle to be overcome in the heterogenation of the metallocene/methylaluminoxane systems.

It has been found that very high ratios of aluminum (methylaluminoxane) to transition metal (metallocene) are required to shift the equilibrium [eq. (1)] from inactive metallocene or even cationic[17] metallocene–aluminum precursor complex in the direction of the catalytically active complex.[18,19]

$$Cp_2MX_2 + n\,MAO \rightleftharpoons \{(Cp_2MX_2)(MAO)_n\}^{\ddagger}_{homogeneous} \quad (1)$$

Many zirconocene systems described in the literature require Al : Zr ratios on the order of 1000 : 1 to achieve a reasonable activity. The record-high activities for the ethylene polymerizations reported by Kaminsky et al. are usually obtained with ratios of Al : Zr = 15000 : 1 and higher.[4a,18,20] Although there is a report that approximately 90% of the expensive aluminoxane can be replaced with traditional alkylaluminum cocatalysts—with little effect on the catalyst performance towards ethylene[21]—the problem remains to adsorb the catalytically active complex on (e.g.) a silica surface.[16] Transfer of the active complex from the homogeneous to the heterogeneous phase not only leads to diffusion problems for the monomer through the aluminoxane matrix, but the precipitation process leads to a *heterogeneous active complex* with a different activity than the homogeneous analog.

We therefore considered the use of solid methylaluminoxane as a support material. Since simple solvent removal and drying of a MAO–toluene solution leaves the methylaluminoxane as a glassy solid, we had to create a solidification process which yields a porous high surface area MAO material. This article discusses the interaction of methylaluminoxane with α,ω-diols and the reaction of trimethylaluminum with hydrogel as well as attempts to elucidate the product structure by CP/MAS-^{13}C solid-state NMR, scanning electron microscopy, and surface area and porosity studies.

The hydrogel (sometimes also termed aquagel or alcogel) used here represents a specific step in the reaction of water glas with mineral acids which would eventually lead to silica gel. Hydrogel represents a polycondensate of spherical polysilicic acids ($H_mSi_nO_p$ aggregates which are ca. 10 nm in diameter) with numerous waterfilled pores. The water content in this three dimensional network ranges from 65 up to 90% (by weight) in the form of coordinated H_2O as well as Si—OH end groups. Drying of this hydrogel at elevated temperatures leads to silica gel (xero gel).[22]

EXPERIMENTAL

Materials

Ethylene (BASF AG) was polymerization grade and used without further purification. $(C_5H_5)_2ZrCl_2$, 1,10-decanediol and 1,6-hexanediol were obtained from Aldrich Chemical Co., hydrogel from BASF.

Methylaluminoxane was purchased from Schering AG (Bergkamen, Germany) as a toluene solution (5.75% in aluminum by weight, density ≈ 0.9 g/mL, average molecular weight of the MAO oligomers = 900–1100 g/mol). Toluene and heptane were refluxed over sodium metal for more than 4 h, followed by destillation under nitrogen. Pentane was dried over Na/Pb alloy and distilled under nitrogen.

All experiments were carried out with standard Schlenk and vacuum techniques under inert gas (argon, nitrogen). Specific surface areas were determined in the BASF analytical laboratories according to the BET method.

Reaction of MAO with 1,10-Decanediol in the Presence of Tetrahydrofuran (THF)

Experiment A

In a typical reaction 0.70 g of 1,10-decanediol (4.0 mmol) dissolved in 30 mL of THF were added dropwise to 20 mL of the above MAO solution (ca. 40 mmol Al; ratio Al : OH = 5 : 1) diluted by 40 mL of toluene. Gel particles were formed immediately accompanied by gas evolution in an exothermic reaction. At the end a highly viscous slurry was obtained. The solvent was removed *in vacuo* and the precipitate dried at 110°C to yield 2.5 g of a white powder.

The experiment was repeated with Al : OH ratios of 2.5 : 1 and 12.5 : 1.

Experiment B

As described in experiment A 1,10-decanediol was reacted with methylaluminoxane. After completion of the diol addition, however, 50 mL of heptane were added slowly to give a voluminous white precipitate which could be separated from the solvent via filtration through a fritted funnel. After washing with another 50 mL portion of heptane, followed by 30 mL of pentane, the residue was dried *in vacuo* at room temperature (yield 2.2 g).

Reaction of MAO with 1,6-Hexanediol in the Presence of THF

As described before in experiment A and B, 1,6-hexanediol was reacted with MAO at Al : OH ration of 2.5 : 1, 5 : 1, and 12.5 : 1.

Reaction of MAO with 1,10-Decanediol in a THF-Free Medium

Experiment C

To 0.70 g (4.0 mmol) of 1,10-decanediol suspended in 50 mL of toluene were added 20 mL of the MAO solution (ca. 40 mmol Al; Al : OH ratio = 5 : 1). A slow gas evolution could be observed at the surface of the diol particles. After stirring of 1.5 h at room temperature, a slight precipitation had occured but the major amount of the undissolved diol remained unreacted. Subsequent heating to reflux for 2.5 h lead to a gel-like precipitate from which the toluene is distilled off *in vacuo* at 90°C to yield a white powder.

The experiment was repeated with an Al : OH ratio of 10 : 1.

Reaction of Hydrogel with Trimethylaluminum

To a slurry of finely powdered hydrogel (1.8 g) in 50 mL of heptane, cooled to −78°C, were added 100 mL of a 1 *M* solution of $AlMe_3$ in heptane. The mixture is allowed to warm to room temperature and stirred for 10 h to give a white powder. The supernatent liquid is decanted, the residue washed twice with 40 mL of heptane and dried *in vacuo* (yield 3.0 g).

ANAL., Found: Al, 38.8%; Si, 4.2%; C, 8.2%.

The experiment was repeated twice with refluxing the reaction mixture for 2 h after it had been warmed to room temperature.

ANAL., Found: Al, 38.0/33.5%; Si, 4.6/5.7%; C, 6.5/7.9%.

Solid-State NMR Measurements

^{13}C CP/MAS Solid-State NMR Spectra

These were recorded at 75.47 MHz on a Bruker CXP300 spectrometer equipped with a double-bearing probe head. The ceramic rotors (7 mm o.d.) were filled inside a glove-box and driven by nitrogen to ensure anaerobic and anhydrous conditions. Spinning speed was 4 kHz. A contact of 3 ms generated the signal with rf field-strength set to a 4 μs 90° pulse length in both channels, during cross-polarization as well as during decoupling. 20,000 FIDs of

25 ms length were accumulated at 2 s intervals. Nonquaternary suppression (NQS) spectra were run with a dephasing period of 40 μs. Chemical shifts are given with adamantane as an external standard, setting its low field signal to 38.07 ppm.

^{27}Al MAS/NMR Spectra

These were recorded at 78.2 MHz on a Bruker MSL300 spectrometer using double bearing rotors of 4 mm o.d. which were spun at 7 kHz. Direct excitation by a 0.6 μs pulse which corresponded to a 15° flip was used to accumulate at least 10^4 FIDs with a spectral width of 125 kHz (4 μs dwell time). The delay between the single shots was set to 0.5 s without loss of signal. Dipolar decoupling proved unnecessary and was therefore turned off.

Scanning Electron Microscopy

The precipitation of the reaction products was done in a glove-box within an atmosphere of dry nitrogen. After drying the precipitates under nitrogen the samples were transfered to a sputter coater and sputtered with a 10 nm Au/Pd layer to avoid surface charging during SEM observation. SEM investigations were done in a Zeiss SEM (DSM960).

RESULTS AND DISCUSSION

The *methylaluminoxane oligomers react with aliphatic diols* under the evolution of methane gas and the formation of three dimensional lattices. This is schematically depicted in Figure 1.

If the diol is dissolved in THF, the reaction proceeds smoothly at room temperature, giving initially a gel-like fluffy solid in solution from which a free-flowing white powder could be separated upon drying. In toluene, 1,10-decanediol and 1,6-hexanediol have a very low solubility at room temperature. The heterogeneous reaction proceeds only very slowly—possibly does not progress beneath the surface layer—and most of the solid diol is still present after stirring for 2 h at room temperature. Refluxing the toluene is accompanied by melting of the diol (melting point of 1,10-decanediol 72–75°C, 1,6-hexanediol 41–43°C) which then reacts readily with the methyl–aluminum bonds. At our highest Al : OH ratio of 12.5 : 1, the material obtained had more a glassy solid (much like dried MAO) instead of a powder appearance.

A *^{13}C solid-state NMR* investigation of the MAO–diol reaction products shows that the carbon chain of the diol does not possess any conformational order but considerable segment mobility, instead, as could be expected for an amorphous framework. This conclusion could be drawn from the observation of the inner chain carbons (e.g., C^2—C^9 in decanediol) upon direct excitation whereas the (Al—O)—CH_2 atom in the vicinity of the Al junction (C^1, C^{10}) at ca. 64 ppm is comparatively rigid. The diol signals in the MAO adduct are slightly shifted with respect to the crystalline educt (cryst. decanediol 62.9, 33.6, and 28.4 ppm versus 63.2, 31.9, and 25.5 ppm in the adduct).

The samples from experiment A—reaction of MAO and diol in toluene/THF, followed by drying at elevated temperature—show, in addition to the above alcoholic methylene at around 64 ppm, another —CH_2—O-signal at somewhat lower field [around 71 ppm; see Fig. 2 (spectrum 1)]. This signal was only weakly present in probes from experiment B—reaction of MAO with diol in toluene/THF, followed by addition of heptane and drying at room temperature [see Fig. 2 (spectrum 2)] and it was absent in the sample from experiment C—reaction of MAO with diol in a THF-free medium [see Fig. 2 (spectrum 3)].

The —CH_2—O signal at 71 ppm relaxes faster than the alcoholic methylene at 64.4 ppm and responds weaker to an interruption of the dipolar decoupling (CP, NQS = nonquartenary suppression). Both indicate a higher mobility of the structure in question. Such could be expected from unreacted —CH_2—OH end groups of the diol. (The shift in the signal position from the pure crystalline diol could have been explained with the loss of the crystalline structure in the MAO–diol and the missing hydrogen bonding.) This first attempt to explain the signal at 71 ppm was, however, quickly abondoned when we recognized that the intensity of the peak at 64 ppm (Al—O—CH_2—) was constant relative to the other diol—CH_2— signals (around 30 ppm) and corresponded to the expected ratio of 2 : 8 (for decanediol). In other words, the intensity of the signal at 64 ppm did not decrease in favor of the 71 ppm peak; thus, the latter could not be related to the diol. Instead, the 71 ppm signal paralleled the intensity of a peak at 25.4 ppm.

It remains to be discussed if the signal at 71 ppm could have originated from the tetrahydrofuran solvent. This is supported by the fact that a sample from experiment C—synthesized in a THF-free reaction—does not contain this puzzling signal [Fig. 2 (spectrum 3)]. In a control measurement the probe

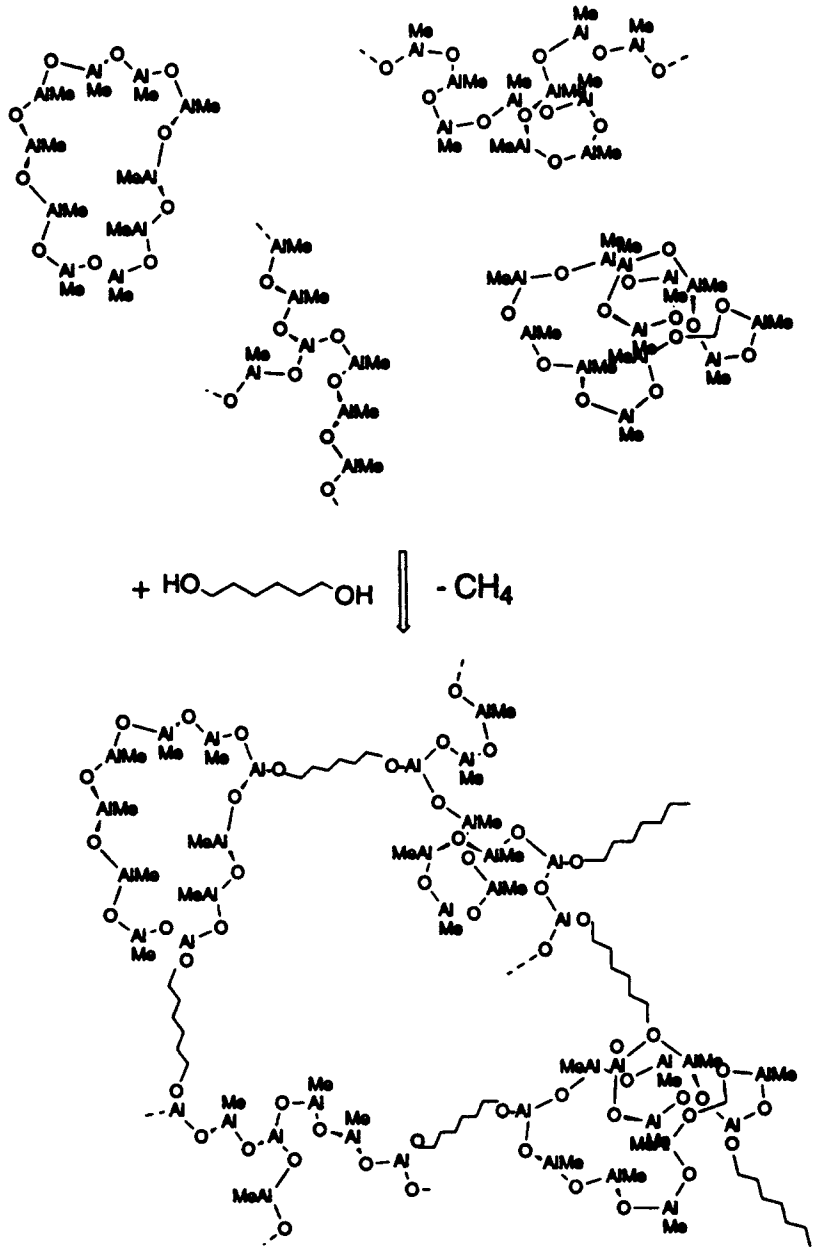

Figure 1. Schematic representation of the MAO–oligomer reaction with aliphatic diols to give three-dimensional lattices.

from experiment C was stored in THF vapor and the spectrum rerun. Tetrahydrofuran is indeed absorbed by the sample and effectively coordinated so that the THF signals (at 67.5 and 25.4 ppm) are observed with a cross-polarization pulse sequence [see Fig. 2 (spectrum 5)]. However, the THF signal at 67.5 ppm lies at somewhat higher field (smaller ppm values) than the peak in question at 71 ppm. Furthermore, the THF signal is considerably sharper due to its higher mobility.

We, therefore, propose that the peak at 71 ppm is not due to monomeric THF, but can most likely be ascribed to polymeric tetrahydrofuran. If this interpretation is correct then the polymerization does not take place upon a simple exposure of a MAO–diol adduct to THF vapor, but requires heating of the sample—as was the case in experiment A. This is consistent with the observation that only a very weak polytetrahydrofuran signal could be detected under the comparatively mild work-up conditions of experiment B, despite the use of a toluene/THF reaction medium just as in A.

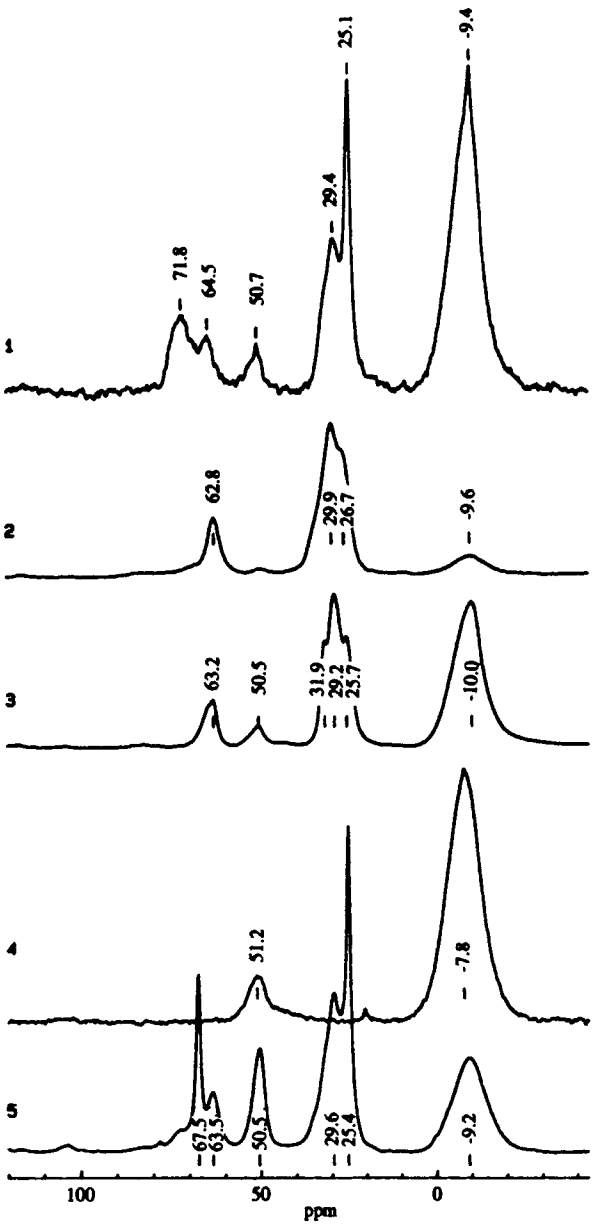

Figure 2. ^{13}C CPMAS spectrum of: (1) the MAO-1,10-decanediol adduct synthesized in toluene/THF and dried at 100°C (experiment A; Al : OH = 12.5 : 1); (2) the MAO-1,10-decanediol adduct synthesized in toluene/THF, precipitated/washed with heptane, and dried at room temperature (experiment B; Al : OH = 2.5 : 1); (3) the MAO-1,10-decanediol adduct synthesized in refluxing toluene (THF-free; experiment C; Al : OH = 5 : 1); (4) a solid methylyluminoxane sample; (5) the sample from spectrum 3 after exposure to THF vapor.

The ^{13}C solid-state NMR spectrum of the solvent-free, pure commercial methylaluminoxane [Fig. 2 (spectrum 4)] consists of a relatively broad signal for the methyl groups at −7.8 ppm. The peak position is expected for Al–CH_3. The line width is probably due to the coexistence of different structural types in this fluxional oligomer (cf. **1**, **2**). Besides the methyl carbon there is, however, a second signal clearly visible at ca. 51 ppm. We are confident that this peak can be assigned to —OCH_3 bonded to aluminum. The area ratio of —OCH_3 to —CH_3 is about 1 : 9. The methoxy signal is also present in all of the above MAO–diol adducts and rises strongly upon exposure to air (i.e., dioxygen). Thus, one should be aware of a possible partial oxidation of Al–CH_3 to Al–OCH_3 in methylaluminoxane samples.

An attempt was also made to gain insight into the structure of the MAO–diol adducts with the help of ^{27}Al MAS NMR: All samples investigated show a broad, little structured ^{27}Al nuclear magnetic resonance spectrum with maxima at 64, 30, and 7 ppm, shown in Figure 3.

In view of the high aluminum content of the probes, the signal intensity is relatively small, thereby indicating that only a minor part of the aluminum had been actually detected in this spectrum.

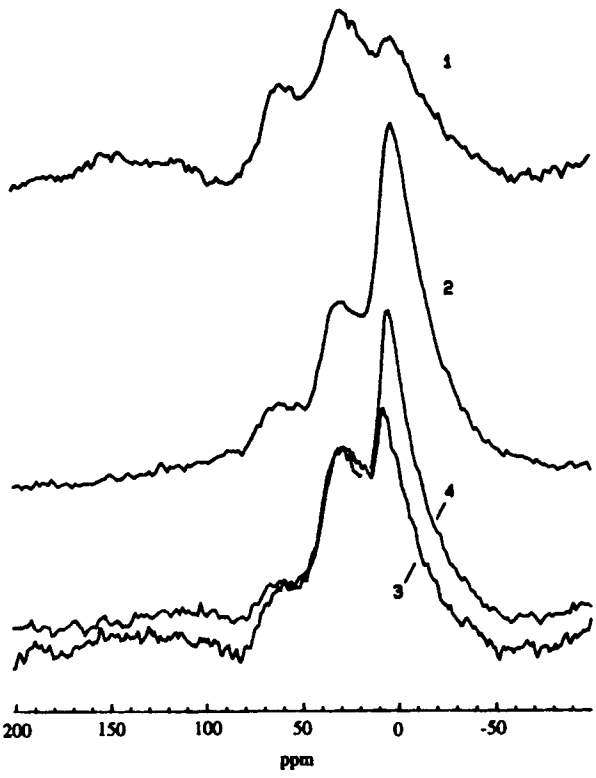

Figure 3. ^{27}Al MAS spectrum of: (1) solid MAO; (2) the MAO-1,10-decanediol adduct synthesized in toluene/THF, precipitated/washed with heptane and dried at room temperature [experiment B; Al : OH = 2.5 : 1; cf. spectrum (2) in Fig. 2]; (3) the MAO-1,10-decanediol adduct synthesized in toluene/THF and dried at 100°C [experiment A; Al : OH = 12.5 : 1; cf. spectrum (1) in Fig. 2]; (4) the sample from spectrum 3 after exposure to THF vapor.

The major percentage obviously gave such a broad line that vanished in the base line. The signal intensity can be enhanced, however, with the uptake of toluene from a sample exposure to toluene vapor. The solvent molecules create a larger number of symmetric aluminum environments, preferentially with an octahedral coordination (ca. 0 ppm). The signal at 7 ppm belongs to Al in an octahedral environment. Its share in the spectrum—relative to MAO—also increases upon reaction with the diol.

Together, these findings lead us to conclude that there is predominantly a nonspherical, i.e., a nontetrahedral or nonoctahedral, charge distribution around the aluminum in methylaluminoxane or its reaction products. A nonspherical charge distribution leads to an electric field gradient (EFG) at the nucleus, and in turn to rather broad signals for quadrupole nuclei, such as ^{27}Al. Thus, no conclusions can be drawn concerning the structural chemistry of the sample. The nuclear magnetic resonance position in the solid state is primarily determined through the symmetry around the aluminum.

Scanning electron microscopy (SEM) studies of the amorphous solids obtained from the reaction of MAO with the diols revealed that the microstructure down to 500 nm is very similar for both 1,6-hexanediol and 1,10-decanediol as a linking agent, as well as for varying the Al : OH ratio from 2.5 to 5 : 1. Figure 4 shows the electron micrographs of a typical product example.

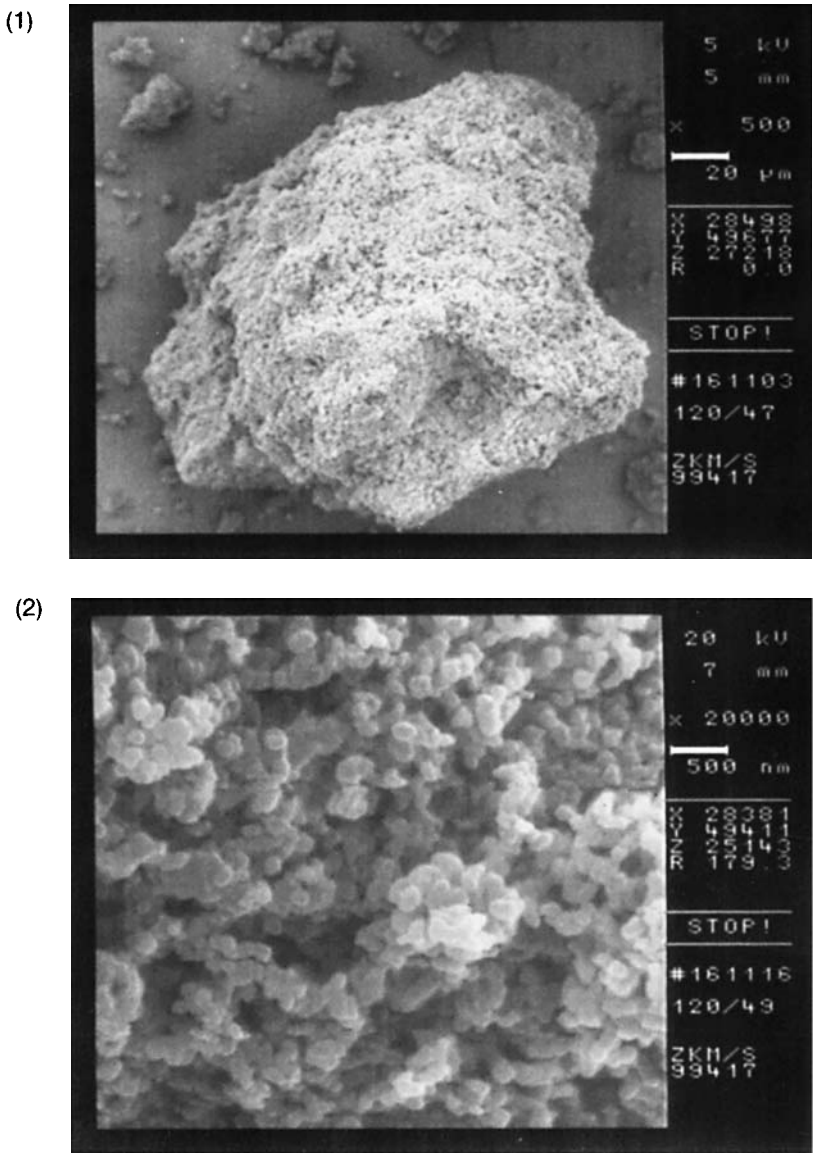

Figure 4. SEM picture of MAO–diol adducts (experiment A with 1,10-decanediol and Al : OH = 5 : 1): (1) view of a powder particle; (2) surface view.

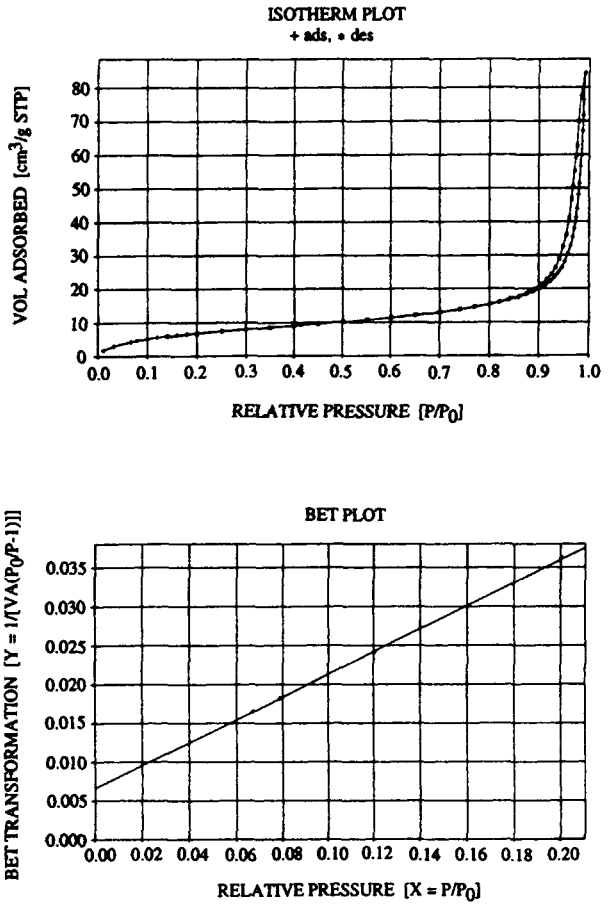

Figure 5. (a) BET adsorption/desorption isotherm for a MAO–1,6-hexanediol adduct (experiment A; Al : OH = 2.5 : 1); (b) BET plot for (a).

It is evident that the material, a conglomerate of ca. 100 nm particles, has a porous surface. Although the MAO–diol composites with Al : OH ratios from 2.5 to 5 : 1 seem to be handable in air without an immediately visible macroscopic decomposition, the SEM investigation (not pictured here) revealed the reactive nature of the material. A nonporous crust forms rapidly at the surface upon hydrolysis.

The *specific surface area* according to the Brunauer, Emmett, and Teller (BET) theory[23] was determined on selected MAO–diol adducts from experiment A. Figure 5(a) shows an example of the experimentally obtained adsorption (and desorbtion) isotherm from which the BET plot [Fig. 5(b)] is constructed in the range $0.05 \leq P/P_0 \leq 0.20$. From the slope, s, and the intercept, i, of the straight line in this BET plot, the total (BET) surface area and BET constant ($C = s/i + 1$) can be calculated. Table I lists the relevant calculational parameters for the samples investigated.

The shapes of the adsorption isotherms [cf. Fig. 5(a)] for all four probes are of type II—in agreement with the BET constant larger than 2.[23] A type II isotherm implies that adsorption occurs on nonporous powders or on powders with pore diameters larger than micropores. The inflection point or knee of the isotherm (here at about 0.5 relative pressure) lies usually near the completion of the first adsorbate monolayer. With increasing relative pressure, second and higher layers are completed until the number of adsorbed layers becomes infinite at saturation. For $P/P_0 \geq 1$ condensation of the adsorbate occurs. From the calculation parameters in Table I, no large changes are apparent upon variation of the diol component or the Al : OH ratio.

Pore size distributions are usually measured using the desorption isotherm included in Figure 5(a). Here the data was evaluated according to the Barrett, Joynes, and Halenda (BJH) numerical integration method.[23] The parameters thus obtained, such as BJH cumulative desorption surface area of pores, the pore volume, and average pore diameter are included in Table I.

Table I. BET and BJH Parameters for MAO–Diol Adducts Obtained in Experiment A

Diol	Al : OH Ratio	Slope[a]	Y Intercept[a]	BET Constant	BET Surface Area[a] (m^2/g)	BJH Surface Area (S) of Pores (m^2/g)	Pore Volume (V) (cm^3/g)	Average Pore Diameter ($4\ V/S$) (Å)
Decanediol	5 : 1	0.201 (2)	0.0079 (2)	26.43	20.9 (2)	18.85	0.218	463
	2.5 : 1	0.2049 (8)	0.0095 (1)	22.58	20.30 (7)	18.29	0.133	291
Hexanediol	5 : 1	0.1197 (4)	0.00595 (6)	21.12	34.6 (1)	36.85 (des.)[b] 29.59 (ads.)[c]	0.204	221
	2.5 : 1	0.147 (2)	0.0066 (2)	23.26	28.4 (3)	24.45	0.119	194

[a] Standard deviation for the last significant figure is given in parenthesis.
[b] The desorption hysteresis loop has not closed here at the low pressure end.
[c] Value from the adsorption isotherm.

The (BJH) surface area of pores is usually less than the BET area (cf. Table I) since it does not include the surface contributed by micropores. Otherwise, the relative variation among the samples tested with different diols and Al : OH ratios is like those seen before from the BET plot evaluation. The calculated pore volumes in Table I vary somewhat with the Al : OH ratios, but not with the diol.

Figure 6(a) shows the pore-size distribution curve prepared from the data of the desorption isotherm in Figure 5(a). Figure 6(b) is the same data plotted as the cumulative pore volume. It is evident that macropores in a rather wide range of 200–1000 Å (20–100 nm) dominate the pore-size distribution.

The *reaction of trimethylaluminum with hydrogel* yields a white powder. The educts were initially brought in contact at −78°C to avoid an uncontrolled reaction. Even at 0°C the reaction was still rather slow, though, and completion of the reaction required stirring of the mixture for more than 12 h at room temperature or refluxing for 2 h until no more gas was evolved, although the clear supernatent liquid still contained reactive trimethylaluminum.

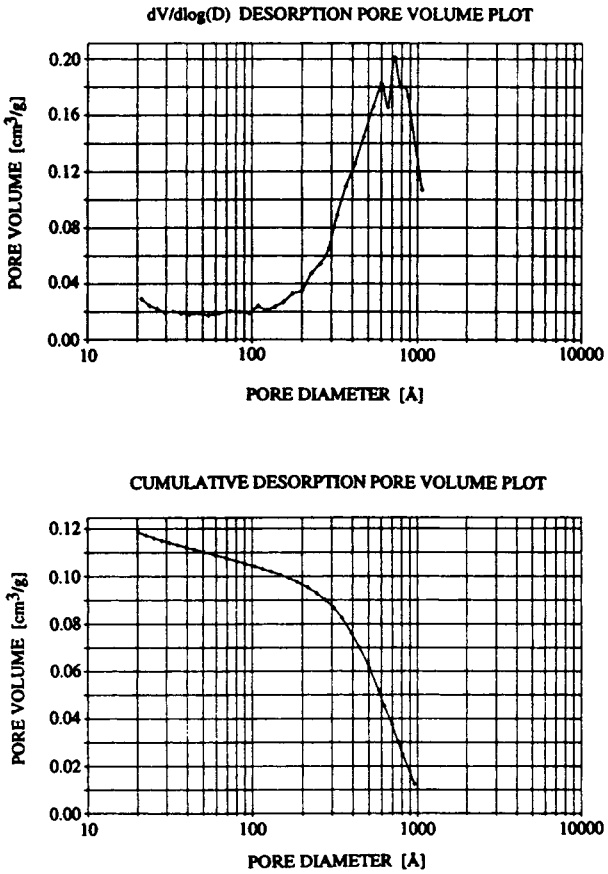

Figure 6. (a) Pore size distribution curve and (b) cumulative pore volume plot, obtained from the desorption isotherm of the MAO–1,6-hexanediol adduct in Figure 5(a).

The white powder formed in the reaction has the expected low silicon content of 4.0–5.7% according to the elemental analyses. However, the aluminum percentage of 32 to 39 in combination with a carbon analysis of 6.5–8% is too high to assign predominantly a methylaluminoxane structure to this material. Instead of a molar Al : C ratio of about 1 : 1 for MAO, the ratio is roughly 2 : 1 in the hydrogel–TMA reaction product, i.e., statistically only every second aluminum atom carries a methyl group. This indicates that all three methyl groups are hydrolized in a large portion of the trimethylaluminum to give $Al(O—)_3$ units, despite relatively mild and careful reaction conditions.

Scanning electron microscopy studies illustrate that in the 500 nm magnification, the microstructure of the hydrogel–TMA adduct (not shown) is very similar to that of the MAO–diol product (see Fig. 4). Hydrogel–TMA also shows the same microscopic crust formation upon contact with air as for the MAO–diol composite.

Preliminary results indicate that the addition of zirconocene dichloride and MAO to the MAO–diol systems gives rise to heterogeneous catalysts for slurry or gas-phase polymerization of ethylene with higher polymer yield on a *per gram catalyst* basis (including the support material) for the MAO–diol support compared to our best silica support.[16] Further studies in this direction are necessary for a more detailed understanding of the support–metallocene interdependencies.

C.J. carried out part of this work during a postdoctoral stay at BASF AG, Ludwigshafen. He thanks BASF for a fellowship and Abteilungsdirektor Dr. G. Schweier for his support and interest in the work. We thank Dr. Bröcker for obtaining the BET analytical data.

REFERENCES AND NOTES

1. (a) K. H. Reichert and K. R. Meyer, *Makromol. Chem.*, **169**, 163 (1973); (b) W. P. Long, and D. S. Breslow, *Liebigs Ann. Chem.*, 463 (1975).
2. (a) A. Andresen, H.-G. Cordes, J. Herwig, W. Kaminsky, A. Merck, R. Mottweiler, J. Pein, H. Sinn, and H. Vollmer, *Angew. Chem.*, **88**, 689 (1976); *Angew. Chem. Int. Ed. Engl.*, **15**, 630 (1976); (b) J. Cihlar, J. Mejzlík, and O. Hamrík, *Makromol. Chem.*, **179**, 2553 (1978).
3. For a review on aluminoxanes, see: S. Pasynkiewicz, *Polyhedron*, **9**, 429 (1990).

4. (a) H. Sinn, W. Kaminsky, H.-J. Vollmer, and R. Woldt, *Angew. Chem.*, **92,** 396 (1980); *Angew. Chem. Int. Ed. Engl.*, **19,** 390 (1980); (b) H. Sinn and W. Kaminsky, *Adv. Organomet. Chem.*, **18,** 99 (1980).
5. (a) F. R. W. P. Wild, L. Zsolnai, G. Huttner, and H. H. Brintzinger, *J. Organomet. Chem.*, **232,** 233 (1982); (b) F. R. W. P. Wild, M. Wasiucionek, G. Huttner, and H. H. Brintzinger, *J. Organomet. Chem.*, **288,** 63 (1985).
6. W. Kaminsky, K. Külper, H. H. Brintzinger, and F. R. W. P. Wild, *Angew. Chem.*, **97,** 507 (1985); *Angew. Chem. Int. Ed. Engl.*, **24,** 507 (1985).
7. D. Cam, E. Albizzati, and P. Cinquina, *Makromol. Chem.*, **191,** 1641 (1990).
8. L. Resconi, S. Bossi, and L. Abis, *Makromolecules,* **23,** 4489 (1990).
9. L. A. Nekhaeva, G. N. Bondarenko, S. V. Rykov, A. I. Nekhaev, B. A. Krentsel, V. P. Marin, L. I. Vyshinskaya, I. M. Khrapova, A. V. Polonskii, and N. N. Korneev, *J. Organomet. Chem.*, **406,** 139 (1991).
10. G. Erker, M. Albrecht, S. Werner, and C. Krüger, *Z. Naturforsch.*, **45b,** 1205 (1990).
11. J. C. W. Chien and R. Sugitomo, *J. Polym. Sci. Part A: Polym. Chem.*, **29,** 459 (1991).
12. S. van der Ven, *Polypropylene and Other Polyolefins: Polymerization and Characterization,* Elsevier, Amsterdam, 1990. p. 43.
13. H.-F. Herrmann and L. L. Böhm, *Polym. Commun.*, **32,** 58 (1991), and references therein.
14. T. E. Nowlin, R. I. Mink, F. Y. Lo, and T. Kumar, *J. Polym. Sci. Part A: Polym. Chem.*, **29,** 1167 (1991).
15. Attempts towards the "heterogenation" of metallocene catalysts are largely described in the patent literature, e.g., (a) U.S. Pat. 4,914,253 A (Exxon, 5/90); *Chem. Abstr.*, **113:** 98282t; (b) Eur. Pat. 0368644 (Exxon, 5/90); *Chem. Abstr.*, **113:** 153268v; (c) WO 89/09237 A1 (Exxon, 10/89); *Chem. Abstr.*, **112:** 99482z; (d) Eur. Pat. 323716 A1 (Exxon, 5/90); *Chem. Abstr.*, **111:** 233880n; (e) Eur. Pat. 0293815 (Hoechst, 12/88); *Chem. Abstr.*, **111:** 195585k.

Examples of journal publications can be found in: (a) T. Tsutsui and N. Kashiwa, *Polymer,* **32,** 2671 (1991); (b) J. C. W. Chien, and D. He, *J. Polym. Sci. Part A: Polym. Chem.*, **29,** 1603 (1991); (c) K. Soga, J. R. Park, and T. Shiono, *Polym. Commun.*, **32,** 310 (1991).

16. C. Janiak and B. Rieger, *Angew. Makromol. Chem.*, submitted.
17. R. F. Jordan, *J. Chem. Ed.*, **65,** 285 (1988); R. F. Jordan, P. K. Bradley, R. E. LaPointe, and D. F. Taylor, *New J. Chem.*, **14,** 505 (1990), and references therein.
18. B. Rieger and C. Janiak, *Angew. Makromol. Chem.*, submitted.
19. See for comparison: K. Meyer, and K. H. Reichert, *Angew. Makromol. Chem.*, **12,** 175 (1970); G. Fink and W. Zoller, *Makromol. Chem.*, **182,** 3265 (1981).
20. (a) W. Kaminsky, M. Miri, H. Sinn, and R. Woldt, *Makromol. Chem. Rapid Commun.*, **4,** 417 (1983); (b) W. Kaminsky, K. Külper, and S. Niedoba, *Makromol. Chem. Makromol. Symp.*, **3,** 377 (1986); (c) W. Kaminsky and M. Schlobohm, *Makromol. Chem. Makromol. Symp.*, **4,** 103 (1986).
21. J. C. W. Chien and B.-P. Wang, *J. Polym. Sci. Part A: Polym. Chem.*, **26,** 3089 (1988).
22. (a) A. F. Holleman and E. Wiberg, *Lehrbuch der Anorganischen Chemie,* 91st–100th ed., de Gruyter, Berlin, 1985. p. 763. (b) A comprehensive treatment can be found in: R. K. Iler, *The Chemistry of Silica. Stability, Polymerization, Colloid and Surface Properties, and Biochemistry,* Wiley, New York, 1979.
23. (a) S. Lowell, J. E. Shields, *Powder Surface Area and Porosity,* 2nd ed., Chapman and Hall, London, 1984, and references therein; (b) S. Lowell, *Introduction to Powder Surface Area,* Wiley, New York, 1979.

Received September 15, 1992
Accepted April 13, 1993